

Subgap in the surface bound states spectrum of Superfluid $^3\text{He-B}$ with Rough Surface

Y. Nagato,* S. Higashitani, and K. Nagai

*Graduate School of Integrated Arts and Sciences, Hiroshima University,
Kagamiyama 1-7-1, Higashi-Hiroshima, 739-8521 Japan*

Subgap structure in the surface bound states spectrum of Superfluid $^3\text{He-B}$ with rough surface is discussed. The subgap is formed by the level repulsion between the surface bound state and the continuum states in the course of multiple scattering by the surface roughness. We show that the level repulsion is originated from the nature of the wave function of the surface bound state that is now recognized as Majorana Fermion. We study the superfluid $^3\text{He-B}$ with a rough surface and under magnetic field perpendicular to the surface using the quasi-classical Green function together with random S-matrix model. We calculate the self-consistent order parameters, the spin polarization density and the surface density of states. It is shown that the subgap is found also under the magnetic field perpendicular to the surface. Magnetic field dependence of the transverse acoustic impedance is also discussed.

Keywords: superfluid ^3He , surface bound state, Majorana Fermion, magnetic field, rough surface, transverse acoustic impedance

I. INTRODUCTION

Since the discovery of superfluid ^3He , it has been well known that the superfluid state of unconventional pairing states is significantly affected by the presence of surface.[1] The order parameter is suppressed near the boundary within some coherence lengths and the surface density of states is considerably modified from the bulk behavior. Such surface effects are caused by the surface scattering and depend upon the nature of boundary condition, whether quasi-particle scattering is specular or diffusive.

Typical example of the surface effects is the formation of surface bound states with energy below the bulk energy gap. [2–5] Buchholtz and Zwicknagl[2] found mid-gap states in the BW state with a specular surface. Hara and Nagai[3] showed that p -wave polar state with a specular surface always has zero energy surface bound states irrespective of the direction of the Fermi momentum. Zhang[4] discussed the effect of surface roughness on the surface density of states of superfluid $^3\text{He-B}$. Surface bound states in superfluid $^3\text{He-B}$ are now recognized as Majorana Fermions reflecting the topological property of the bulk system.[6–8] A comprehensive review from this aspect has been recently given by Mizushima et al.[9]

Experimental observation of the surface bound states in superfluid ^3He was not performed because of the lack of appropriate surface probe for the neutral superfluid. It has been recently reported, [5, 10–13] however, that the transverse acoustic impedance provides useful information on the surface bound states in the B phase of superfluid ^3He . The key point to identify the surface bound states is the existence of the subgap in the surface density of states.[4, 14, 15] When the surface is specular, the surface density of states is filled by the bound states up to the bulk energy gap Δ_b . In the presence of rough surface, however, the bound state energies are lowered and have a maximum Δ^* below the bulk energy gap Δ_b . As a result, there occurs a subgap between Δ^* and Δ_b . The pair excitations give rise to a typical cusp in the real part of the transverse acoustic impedance and a peak in the imaginary part at the frequency $\Delta^* + \Delta_b$, which was observed by Aoki et al.[10]

The subgap structure in the surface density of states of $^3\text{He-B}$ was first reported by Zhang[4], who calculated the surface density of state using the quasi-classical theory with thin dirty layer model. It was confirmed by later calculations using other rough surface models.[14, 15] However, the origin of the subgap structure has been a puzzle, although Zhang[4] had suggested that it might be related to the suppression of the parallel component of the order parameter near the surface by the roughness. In Ref.16, we found the same subgap structure also in two-dimensional chiral superconducting state which has a full gap at the Fermi surface as $^3\text{He-B}$. We showed that the origin of the subgap is the level repulsion between the bound state and the continuum states.

In this paper, we show that the subgap in the surface density of states exists in superfluid $^3\text{He-B}$ also in the presence of magnetic field perpendicular to the surface and that the level repulsion is originated from the structure of the bound state wave function that ensures the surface bound state to be Majorana Fermion.

* nagato@riise.hiroshima-u.ac.jp

This paper is organized as follows. In the next section, we discuss the possible form of the wave function (Nambu amplitude) of the surface bound state allowed by the symmetry of the Hamiltonian. All the previous results[17–21] of the bound state wave function agree with this possible form. In section III, we consider the quasi-classical Green function for superfluid $^3\text{He-B}$ with a plane surface and magnetic field perpendicular to the surface. Rough surface effects are treated using the random S -matrix theory.[22, 23] This theory is a self-consistent Born approximation theory with respect to the surface scattering and includes a roughness parameter W ($0 \leq W \leq 1$). The specular surface corresponds to $W = 0$ and the fully diffusive surface corresponds to $W = 1$. We can show[5] that the random S -matrix theory with $W = 1$ is equivalent to Ovchinnikov’s rough surface boundary condition.[25, 26] At the surface, we can separate the quasi-classical Green function into two parts. One of them, which we shall call “pole part”, includes the contribution from the surface bound states and the other part, which we shall call “continuum part”, does not. From the structure of the bound state wave function, we show that the “pole part” and the “continuum part” appear alternately in the multi-scattering processes by the surface roughness. This leads to the level repulsion between the bound state and the continuum states. In section IV, we consider a case with weak surface roughness. Using perturbation theory with respect to the roughness parameter W , we show that the bound state energies are lowered by the roughness and show how the upper edge Δ^* appears. Section V is devoted to the self-consistent calculation of the order parameters and the spin polarization density. To perform the numerical calculations, we use the Riccati representation of the quasi-classical Green function. [23, 27–30] Using the self-consistent results, we calculate the surface density of states and show that the well defined subgap structure exists even in the presence of magnetic field. In section VI, we discuss the transverse acoustic impedance and show how it depends on the magnetic field. The final section is devoted to summary and discussion. In the Appendices, Riccati representation of 4×4 quasi-classical Green function is discussed. Explicit expressions for the transverse acoustic impedance is also presented.

II. SURFACE BOUND STATES

Let us briefly review the surface bound states of a superfluid $^3\text{He-B}$ filling $z > 0$ domain with a plane surface located at $z = 0$. [5, 17–21] The magnetic field is applied in the direction perpendicular to the plane surface. We consider 4-dimensional Bogoliubov equation

$$\int d\mathbf{r}' \mathcal{H}(\mathbf{r}, \mathbf{r}') \Psi(\mathbf{r}') = E \Psi(\mathbf{r}), \quad (1)$$

where Ψ is the Nambu amplitude and the Hamiltonian of the system in 4-dimensional Nambu representation is given by

$$\mathcal{H}(\mathbf{r}, \mathbf{r}') = \begin{pmatrix} \xi(\nabla) \delta(\mathbf{r} - \mathbf{r}') & \Delta(\mathbf{r}, \mathbf{r}') \\ \Delta^\dagger(\mathbf{r}', \mathbf{r}) & -\xi(\nabla) \delta(\mathbf{r} - \mathbf{r}') \end{pmatrix} - h \begin{pmatrix} \sigma_z & \\ & -\sigma_z \end{pmatrix} \delta(\mathbf{r} - \mathbf{r}'), \quad (2)$$

where $\xi(\nabla) = \frac{\nabla^2}{2m^*} - \mu$ is the quasi-particle energy measured from the Fermi surface and h is half the Larmor frequency ω_L . The order parameter of $^3\text{He-B}$ of the present system is

$$\Delta(\mathbf{r}, \mathbf{r}') = \sum_{\mathbf{p}} e^{i\mathbf{p} \cdot (\mathbf{r} - \mathbf{r}')} \Delta(z, \hat{\mathbf{p}}) \quad (3)$$

$$\Delta(z, \hat{\mathbf{p}}) = \begin{pmatrix} -d_x + id_y & dz \\ dz & d_x + id_y \end{pmatrix} = \begin{pmatrix} -\Delta_t e^{-i\phi} & \Delta_\ell \\ \Delta_\ell & \Delta_t e^{i\phi} \end{pmatrix}, \quad (4)$$

$$\Delta_t = \Delta_{\parallel}(z) \sin \theta, \quad (5)$$

$$\Delta_\ell = \Delta_{\perp}(z) \cos \theta \quad (6)$$

where \mathbf{d} is the d -vector, $\hat{\mathbf{p}}$ is a unit vector along \mathbf{p} and θ, ϕ are the polar and the azimuthal angle of \mathbf{p} .

Let us consider the bound state wave function. Since the momentum component \mathbf{K} parallel to the surface is conserved when the surface is specular, we consider the Nambu amplitude of the form

$$\Psi(\mathbf{r}) = e^{i\mathbf{K} \cdot \mathbf{r}} \sum_{\alpha=\pm} \Phi_{\alpha}(z) e^{i\alpha k z}, \quad (7)$$

with $k = \sqrt{p_F^2 - \mathbf{K}^2}$ the z component of the Fermi momentum. Making use of the rotational symmetry around the z -axis, we rotate the spin axis so that \mathbf{d} is along the y direction. Applying the WKB approximation on Eq.(1), we

obtain the Andreev equation

$$\mathcal{H}_\alpha \Phi_\alpha = \begin{pmatrix} -i\alpha v_F \cos \theta \partial_z - h\sigma_z & \Delta_\alpha(z) \\ \Delta_\alpha^\dagger(z) & i\alpha v_F \cos \theta \partial_z + h\sigma_z \end{pmatrix} \Phi_\alpha = E\Phi_\alpha, \quad (8)$$

where $v_F = p_F/m^*$ is the Fermi velocity and

$$\Delta_\alpha(z) = \begin{pmatrix} i\Delta_t & \alpha\Delta_\ell \\ \alpha\Delta_\ell & i\Delta_t \end{pmatrix} \quad (9)$$

which satisfies

$$\Delta_\alpha(z)^\dagger = -\Delta_{-\alpha}(z). \quad (10)$$

The surface bound states can be obtained by seeking for damping solutions of Eq.(8) and imposing the boundary condition $\Psi = 0$ at $z = 0$. It is useful to note that \mathcal{H}_α satisfies

$$\rho_2 \sigma_1 \mathcal{H}_\alpha \sigma_1 \rho_2 = \mathcal{H}_{-\alpha}, \quad (11)$$

where ρ_i 's and σ_i 's are Pauli matrices in the particle-hole space and the spin space, respectively. Since the bound state is non-degenerate, it follows that

$$\Phi_-(z) = c \rho_2 \sigma_1 \Phi_+(z), \quad (12)$$

where c is a constant. Substituting this into the boundary condition $\Phi_+(0) = -\Phi_-(0)$, we obtain

$$\Phi_+(0) = u_1 \begin{pmatrix} 1 \\ 0 \\ 0 \\ -ic \end{pmatrix} + u_2 \begin{pmatrix} 0 \\ ic \\ 1 \\ 0 \end{pmatrix} = -\Phi_-(0), \quad c^2 = 1 \quad (13)$$

where u_1, u_2 are constants. From the previous analyses,[17–21] one can conclude that the damping solution is obtained when $c = 1$ (see below). At the surface, therefore, the wave function of the bound state is given by a linear combination of

$$\Phi_\uparrow = \begin{pmatrix} 1 \\ 0 \\ 0 \\ -i \end{pmatrix}, \quad \Phi_\downarrow = \begin{pmatrix} 0 \\ i \\ 1 \\ 0 \end{pmatrix}. \quad (14)$$

When we assume that Δ_\parallel and Δ_\perp are constant, we can find explicit solutions for the bound state.[17, 18] In the absence of magnetic field, we can find both positive and negative energy bound state for each Fermi momentum $\mathbf{p}_F = (\mathbf{K}, k)$. For positive energy eigen value $E = \Delta_\parallel \sin \theta$, the eigen function is given by

$$\Psi_{\mathbf{K}}^{(+)}(\mathbf{r}) = e^{i\mathbf{K}\cdot\mathbf{r}} \sin(kz) e^{-\kappa z} (\Phi_\uparrow - e^{i\phi} \Phi_\downarrow) \quad (15)$$

and for negative energy eigen value $E = -\Delta_\parallel \sin \theta$

$$\Psi_{\mathbf{K}}^{(-)}(\mathbf{r}) = e^{i\mathbf{K}\cdot\mathbf{r}} \sin(kz) e^{-\kappa z} (e^{-i\phi} \Phi_\uparrow + \Phi_\downarrow). \quad (16)$$

with $\kappa = \Delta_\perp/v_F$. Here we have rotated the spin axis back to the original one. In the presence of magnetic field perpendicular to the surface, the bound state energy has a gap

$$E = \pm \sqrt{\Delta_t^2 + \Delta_Z^2}, \quad \Delta_Z = h. \quad (17)$$

We call Δ_Z ‘‘Zeeman gap’’ in this paper. The corresponding eigen function is given by a linear combination

$$a\Psi_{\mathbf{K}}^{(+)}(\mathbf{r}) + b\Psi_{\mathbf{K}}^{(-)}(\mathbf{r}) \quad (18)$$

and a, b are determined by

$$\frac{a}{-he^{-i\phi}} = \frac{b}{E - \Delta_t} \quad (19)$$

The Nambu amplitudes Φ_\uparrow and Φ_\downarrow are the eigen functions of the zero energy surface bound states of the polar state ($\Delta_t = 0$). Treating Δ_t and h as perturbation,[19, 21] one can also show that the bound state in the BW state is given by the linear combination of Φ_\uparrow and Φ_\downarrow . It is to be noted that, in the Nambu amplitudes Φ_\uparrow and Φ_\downarrow , the particle component and the hole component enter with the same weight, which is a basis for the surface bound states to be Majorana Fermions.

III. QUASI-CLASSICAL GREEN FUNCTION IN THE PRESENCE OF MAGNETIC FIELD

In this section, we discuss the quasi-classical Green function of $^3\text{He-B}$ with the plane surface in the $z = 0$ plane and the magnetic field parallel to the z axis.

We consider the quasi-classical Green function $\hat{G}_\alpha(\epsilon, z)$ ($\alpha = \pm 1$) for the Fermi momentum $\mathbf{p}_\alpha = (\mathbf{K}, \alpha k)$. \mathbf{p}_+ and \mathbf{p}_- are the outgoing and the incoming Fermi momentum, respectively. Since the system keeps rotational symmetry around the z axis, we consider \hat{G}_α for $\phi = \pi/2$ ($(\mathbf{K})_x = 0$). Green's function for arbitrary ϕ is obtained by

$$\mathcal{R}^\dagger(\phi)\hat{G}_\alpha\mathcal{R}(\phi), \quad \mathcal{R}(\phi) = \exp(i(\phi - \pi/2)\rho_3\sigma_3/2) \quad (20)$$

The Eilenberger equation for \hat{G}_α is now given by

$$v_F \cos \theta \partial_z \hat{G}_\alpha = i\alpha \left[\hat{G}_\alpha, \mathcal{E}_\alpha(z) \right] \quad (21)$$

$$\mathcal{E}_\alpha = \mathcal{E}_0 + \mathcal{E}_h \quad (22)$$

$$\mathcal{E}_0 = \epsilon\rho_3 + \begin{pmatrix} & \Delta_\alpha \\ \Delta_{-\alpha} & \end{pmatrix} \quad (23)$$

$$\mathcal{E}_h = h\sigma_3\rho_0, \quad (24)$$

where the order parameter Δ_α is given by Eq. (9).

In the bulk region far from the surface, \hat{G}_α is given by[2, 31]

$$\hat{G}_\alpha^{(0)} = \sum_{\sigma=\pm 1} iP_\sigma \frac{\mathcal{E}_\alpha}{E_\sigma}, \quad (25)$$

where P_σ is a projection operator

$$P_\sigma = \frac{1}{2} \left(1 - \sigma \frac{Q}{|Q|} \right), \quad (26)$$

$$Q = \mathcal{E}_0\mathcal{E}_h + \mathcal{E}_h\mathcal{E}_0, \quad (27)$$

$$|Q| = \sqrt{Q^2} = 2h\sqrt{\epsilon^2 - \Delta_t^2}, \quad (28)$$

and

$$E_\sigma = \sqrt{\epsilon^2 - \Delta_t^2 - \Delta_\ell^2 + h^2 - \sigma Q} \quad (29)$$

In the above, we have defined square root such that has positive imaginary part.

When the surface is specular, \hat{G}_+ and \hat{G}_- should satisfy the boundary condition at the surface $z = 0$

$$\hat{G}_+(0) = \hat{G}_-(0) = \hat{G}_s. \quad (30)$$

Using Eqs.(21), (25) and (30), we can determine the quasi-classical Green function of the system with specular surface (see Appendix B). The quasi-classical Green function of present definition satisfies the normalization condition $\hat{G}_\alpha^2 = -1$.

From the symmetrical property of \mathcal{E}_α

$$\rho_2\sigma_1\mathcal{E}_\alpha\sigma_1\rho_2 = -\mathcal{E}_{-\alpha}, \quad (31)$$

we can show that

$$\rho_2\sigma_1\hat{G}_\alpha(z)\sigma_1\rho_2 = -\hat{G}_{-\alpha}(z), \quad (32)$$

therefore

$$\rho_2\sigma_1\hat{G}_s\sigma_1\rho_2 = -\hat{G}_s. \quad (33)$$

Let us consider how the surface bound states contribute to the quasi-classical Green function. For that purpose, it is useful to remind that \hat{G}_s is expressed in terms of the eigen functions Φ_n of the Andreev equation (8) in a form[22–24]

$$\hat{G}_s = \frac{-1}{2v_F \cos \theta} \frac{1}{2\rho_3} \left(\sum_n \frac{\Phi_n(z)\Phi_n^\dagger(0)}{\epsilon - E_n} \Big|_{z=+0} + \sum_n \frac{\Phi_n(z)\Phi_n^\dagger(0)}{\epsilon - E_n} \Big|_{z=-0} \right). \quad (34)$$

Bearing this in mind, we prepare 4 mutually orthogonal Nambu amplitudes

$$|\Phi_1\rangle = \frac{1}{\sqrt{2}}\Phi_\uparrow, \quad |\Phi_2\rangle = \frac{1}{\sqrt{2}}\Phi_\downarrow, \quad |\Phi'_1\rangle = \rho_3\Phi_1, \quad |\Phi'_2\rangle = \rho_3\Phi_2. \quad (35)$$

When we choose them as base vectors and calculate the matrix elements of $g_s = \rho_3\hat{G}_s$, we find that g_s is block diagonalized, i.e.,

$$g_s = \rho_3\hat{G}_s = \sum_{i,j=1,2} (|\Phi_i\rangle\langle\Phi_i|g_s|\Phi_j\rangle\langle\Phi_j| + |\Phi'_i\rangle\langle\Phi'_i|g_s|\Phi'_j\rangle\langle\Phi'_j|) \quad (36)$$

$$\equiv \sum_{i,j=1,2} (|\Phi_i\rangle\langle g_{ij}^{(1)}|\Phi_j| + |\Phi'_i\rangle\langle g_{ij}^{(2)}|\Phi'_j|). \quad (37)$$

This can be proved by noting that $\rho_2\sigma_1|\Phi_1\rangle = -|\Phi_1\rangle$, $\rho_2\sigma_1|\Phi_2\rangle = -|\Phi_2\rangle$ together with Eq.(33).

$$\begin{aligned} \langle\Phi_i|g_s|\Phi'_j\rangle &= \langle\Phi_i|\rho_3\hat{G}_s|\Phi'_j\rangle \\ &= -\langle\Phi_i|\rho_3\rho_2\sigma_1\hat{G}_s\sigma_1\rho_2\rho_3|\Phi_j\rangle \\ &= -\langle\Phi_i|\rho_2\sigma_1\rho_3\hat{G}_s\rho_3\sigma_1\rho_2|\Phi_j\rangle \\ &= -\langle\Phi_i|\rho_3\hat{G}_s\rho_3|\Phi_j\rangle = -\langle\Phi_i|\rho_3\hat{G}_s|\Phi'_j\rangle = 0. \end{aligned} \quad (38)$$

As was emphasized in the previous section, the bound state wave functions at the surface $z = 0$ are given by the linear combination of $|\Phi_1\rangle$ and $|\Phi_2\rangle$. It follows that the bound states appear in $g^{(1)}$, while $g^{(2)}$ has no contribution from the bound states at all. We call $g^{(1)}$ the ‘‘pole part’’ and $g^{(2)}$ the ‘‘continuum part’’, although $g^{(1)}$ has contribution also from the continuum states. From the normalization condition $\hat{G}_s^2 = -1$ we find

$$g^{(1)}g^{(2)} = -1. \quad (39)$$

Let us now consider the rough surface effects using the random S-matrix model.[14, 22, 23]. According to the theory, the Green functions at the surface are given by

$$\hat{G}_\pm = \hat{G}_s + (\hat{G}_s \pm i)\hat{\mathcal{G}}(\hat{G}_s \mp i), \quad (40)$$

$$\hat{\mathcal{G}} = \frac{1}{\hat{G}_s^{-1} - \Sigma}, \quad (41)$$

where Σ is the surface self energy given by

$$\Sigma = 2W \left\langle \frac{1}{2} \left(\hat{\mathcal{G}} + \rho_3\sigma_3\hat{\mathcal{G}}\sigma_3\rho_3 \right) \right\rangle, \quad (42)$$

$$\langle \dots \rangle = 2 \int_0^{\pi/2} d\theta \sin\theta \cos\theta \dots. \quad (43)$$

Here, $W(0 \leq W \leq 1)$ is a parameter which specifies the roughness of the surface; $W = 0$ corresponds to the specular surface and $W = 1$ to the completely diffusive surface.[14, 22, 23] When $W = 1$, the random S-matrix model is equivalent to Ovchinnikov’s boundary condition.[5, 25, 26] Note that Eq.(42) is slightly different from our previous definition $\Sigma = 2W \langle \hat{\mathcal{G}} \rangle$ [14, 22]. This is because the integral over the azimuthal angle ϕ has been already performed (see Eq. (20)).

From the definition of Eq. (42) (see also Eq. (B13)), we can show that Σ is also block diagonalized by the same base vectors as

$$\Sigma = \rho_3 \sum_{i,j=1,2} (|\Phi_i\rangle\langle s_{ij}^{(1)}|\Phi_j| + |\Phi'_i\rangle\langle s_{ij}^{(2)}|\Phi'_j|), \quad (44)$$

where $s^{(1)}$ and $s^{(2)}$ are 2×2 diagonal matrices. We can also show that

$$\mathcal{G} = \frac{1}{\hat{G}_s^{-1} - \Sigma} = \rho_3 \sum_{ij} \left(|\Phi_i\rangle\langle \left(\frac{1}{(g^{(1)})^{-1} - s^{(2)}} \right)_{ij}|\Phi_j| + |\Phi'_i\rangle\langle \left(\frac{1}{(g^{(2)})^{-1} - s^{(1)}} \right)_{ij}|\Phi'_j| \right), \quad (45)$$

where we used Eq. (39) and $|\Phi'_i\rangle = \rho_3|\Phi_i\rangle$. The self energy equation (42) is also separated.

$$s^{(1)} = 2W \left\langle \left(\frac{1}{(g^{(1)})^{-1} - s^{(2)}} \right)_{\text{diagonal}} \right\rangle \quad (46)$$

$$s^{(2)} = 2W \left\langle \left(\frac{1}{(g^{(2)})^{-1} - s^{(1)}} \right)_{\text{diagonal}} \right\rangle \quad (47)$$

The first term in Eq. (45) shows how the bound state energy is modified by the surface roughness. In fact, when we formally expand the first term, we find that

$$g^{(1)} + g^{(1)}s^{(2)}g^{(1)} + g^{(1)}s^{(2)}g^{(1)}s^{(2)}g^{(1)} + \dots, \quad (48)$$

namely, the ‘‘pole part’’ and the ‘‘continuum part’’ appear alternately in the multi-scattering processes by the roughness. It implies that there occurs level repulsion between the bound state and the continuum states. It leads to the existence of a maximum Δ^* of the bound state energy and a subgap between Δ^* and the bulk energy gap. We have shown in Ref.16 that this actually happens in the two-dimensional chiral superconductor.

Finally we consider the surface density of States $D(\epsilon)$ which is calculated from[14]

$$D(\epsilon) = \int_0^{\pi/2} d\theta \sin\theta n(\epsilon, \theta), \quad (49)$$

$$n(\epsilon, \theta) = \frac{1}{4}N(0)\text{Im tr} \left[\rho_3 \frac{1}{2}(\hat{G}_+(\epsilon + i0) + \hat{G}_-(\epsilon + i0)) \right] \quad (50)$$

$$= \frac{1}{4}N(0)\text{Im tr} \left[\frac{1}{(g^{(1)})^{-1} - s^{(2)}} + \frac{1}{(s^{(1)})^{-1} - g^{(2)}} + \frac{1}{(g^{(2)})^{-1} - s^{(1)}} + \frac{1}{(s^{(2)})^{-1} - g^{(1)}} \right], \quad (51)$$

where $N(0)$ is the normal state density of states.

IV. PERTURBATION THEORY

The advantage of the random S -matrix model is that we can treat the surface roughness in a unified way from the specular limit to the diffusive limit. In this section, we consider the surface density of states when the surface roughness is weak, i. e., W is small.

For simplicity, we assume in this section that the order parameters $\Delta_{\parallel}, \Delta_{\perp}$ are spatially constant. In that case, \hat{G}_s at the specular surface is given by[14, 22, 23]

$$\hat{G}_s = \hat{G}_+^{(0)} + (\hat{G}_+^{(0)} + i) \frac{-1}{\hat{G}_+^{(0)} + \hat{G}_-^{(0)}} (\hat{G}_+^{(0)} - i) \quad (52)$$

$$= \hat{G}_-^{(0)} + (\hat{G}_-^{(0)} - i) \frac{-1}{\hat{G}_+^{(0)} + \hat{G}_-^{(0)}} (\hat{G}_-^{(0)} + i). \quad (53)$$

Substituting Eq.(25), we obtain expressions for \hat{G}_s as is shown in Appendix A. We can also calculate explicitly $g^{(1)}$ and $g^{(2)}$ and find that $g^{(1)}$ has poles at

$$\epsilon = \pm \sqrt{\Delta_t^2 + h^2}, \quad (54)$$

while $g^{(2)}$ has no pole. In fact, we obtain a simple result for the traces

$$\text{tr } g^{(1)} = \epsilon \frac{iE_+ \left(1 + \frac{h}{\sqrt{\epsilon^2 - \Delta_t^2}} \right) + iE_- \left(1 - \frac{h}{\sqrt{\epsilon^2 - \Delta_t^2}} \right) - 2\Delta_\ell}{\epsilon^2 - (\Delta_t^2 + h^2)} \quad (55)$$

$$\text{tr } g^{(2)} = \epsilon \frac{iE_+ \left(1 + \frac{h}{\sqrt{\epsilon^2 - \Delta_t^2}} \right) + iE_- \left(1 - \frac{h}{\sqrt{\epsilon^2 - \Delta_t^2}} \right) + 2\Delta_\ell}{\epsilon^2 - (\Delta_t^2 + h^2)}. \quad (56)$$

Let us consider the angle resolved surface density of states $n(\epsilon, \theta)$ in low energy region. When W is small, the pole part contribution to $n(\epsilon, \theta)$ may be written as

$$n(\epsilon, \theta) = \frac{N(0)}{4} \text{Im tr} \left(\frac{1}{(g^{(1)})^{-1} - s^{(2)}} + s^{(1)} \right) \quad (57)$$

When the surface is specular, $W = 0$, therefore $s^{(1)} = s^{(2)} = 0$. We find from Eq.(55) the bound state peaks

$$\begin{aligned} n(\epsilon, \theta) &= \pi N(0) \Delta_\ell |\epsilon| \delta(\epsilon^2 - (\Delta_t^2 + h^2)) \\ &= \frac{\pi N(0) \Delta_\ell}{2} \left(\delta\left(\epsilon - \sqrt{\Delta_t^2 + h^2}\right) + \delta\left(\epsilon + \sqrt{\Delta_t^2 + h^2}\right) \right) \end{aligned} \quad (58)$$

and also a continuous spectrum of the Bogoliubov quasi-particles which begins from the minimum energy $\Delta_\perp - h$. [31] The first correction by W comes from $s^{(1)}$.

$$\text{Im tr } s^{(1)} = \text{Im tr } 2W \langle g^{(1)} \rangle = 8\pi W |\epsilon| \frac{\Delta_\perp}{\Delta_\parallel^2} \sqrt{1 - \frac{\epsilon^2 - h^2}{\Delta_\parallel^2}} \Theta(|\epsilon| - h), \quad (59)$$

where Θ is the theta function. This describes the effects by the scattering of the bound states by the surface roughness.

Now we consider the correction by W to the the first term of Eq. (57), putting $s^{(2)} = 2W \langle g^{(2)} \rangle$, to study how the bound state energy is modified by the surface roughness.

$$n(\epsilon, \theta) = \frac{N(0)}{4} \text{Im tr} \left(\frac{1}{(g^{(1)})^{-1} - 2W \langle g^{(2)} \rangle} \right) \quad (60)$$

Since the numerical calculation is necessary to evaluate $\langle g^{(2)} \rangle$ when the magnetic field is finite, we further simplify the problem by assuming $\Delta_\parallel = \Delta_\perp = \Delta$. The result is shown in Fig. 1.

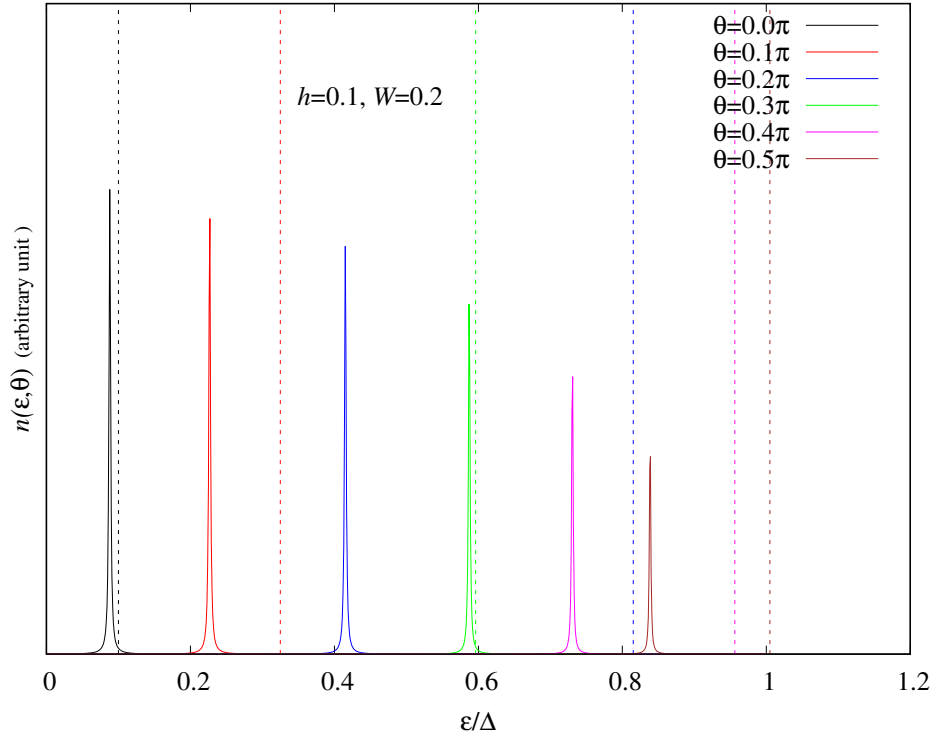


FIG. 1. Bound states contribution to the density of state when $h = 0.1\Delta$ and $W = 0.2$. Artificial width is given to the peaks to show the θ dependence of the spectral weight. The vertical broken lines show the bound state energies when $W = 0$.

Figure 1 shows the bound state contribution to $n(\epsilon, \theta)$ when $h = 0.1\Delta$ and $W = 0.2$. Bound state peaks are artificially broadened to show the θ dependence of the spectral weight. The vertical broken line of the same color shows the bound state energy Eq. (17) when $W = 0$. We find that the bound state energies are shifted to lower energy by the level repulsion with the continuum states. The Zeeman gap Δ_Z is lowered by the roughness. The bound state at $\theta = \pi/2$, which has the maximum energy, has also a lower energy than that in the case of $W = 0$. This energy is Δ^* at the present level of approximation. Important point is that the spectral weight of the bound state peak at Δ^* is finite in contrast to the case of specular surface where the spectral weight is zero when $\theta = \pi/2$ (see Eq. (58)).

The presence of Δ^* should be taken into account in the calculation of $s^{(1)}$ of Eq. (46). Equation (59) of $s^{(1)}$ was obtained by integrating the pole contribution from the bound states over θ . When $W = 0$ the bound state energies extend up to Δ_{\parallel} . But now they are limited below Δ^* . Moreover the spectral weights of the bound states are finite below Δ^* . It follows that there occurs a finite jump to zero in $\text{Im tr } s^{(1)}$ at Δ^* . Bound state contributions to the density of states are, thus, confined in the energy range $\Delta_Z < \epsilon < \Delta^*$, which gives rise to subgap structure,

In addition to the bound states, there is contribution to the density of states from the Bogoliubov quasi-particle excitations which have a minimum energy $\Delta_{\perp} - h$. [31] When W is sufficiently small, Δ^* may merge into this excitation continuum.

In this section, we have discussed using a simplified model. In the following sections, we show the results of more realistic calculations based on the self-consistent order parameter.

V. SELF-CONSISTENT ORDER PARAMETER, SPIN POLARIZED DENSITY AND SURFACE DENSITY OF STATES

In this section we discuss the order parameters, the spin polarization density and the surface density of states of $^3\text{He-B}$ under the magnetic field normal to the rough surface.

The self-consistent order parameter $\Delta(z)$ and the spin polarization density $S_z(z)$ are determined by solving the gap equation

$$\Delta(z, \hat{p}) = \frac{3\pi T \sum_{\omega_n} \int_0^{2\pi} \frac{d\phi_k}{2\pi} \sum_{\alpha}^{\omega_c} \int_0^{\pi/2} \frac{d\theta_k}{2} \sin \theta_k \hat{p} \cdot \hat{k}_{\alpha} \hat{G}_{\alpha}(K, z, i\omega_n) \Big|_{12}}{\ln \frac{T}{T_c} + \sum_{\omega_n > 0}^{\omega_c} \frac{1}{n + 1/2}} \quad (61)$$

and the spin polarization equation

$$S_z(z) = N(0)\tilde{h} - \frac{\pi T N(0)}{4} \sum_{\omega_n}^{\omega_c} \int_0^{\pi/2} d\theta \sin \theta \sum_{\alpha} \text{tr}_{\text{spin}} \left[\sigma_3 \hat{G}_{\alpha}(K, z, i\omega_n) \Big|_{11} \right] \quad (62)$$

where the subscript 11 and 12 mean the 11 and 12 element of the quasi-classical Matsubara Green's function $\hat{G}(i\omega_n)$ in particle-hole space, respectively. The Fermi liquid correction by F_0^a to the effective magnetic field is given by

$$\begin{aligned} \tilde{h} &= \frac{\tilde{\omega}_L}{2} = h - \frac{F_0^a}{N(0)} S_z \\ &= h \left(1 - \frac{F_0^a}{1 + F_0^a} \left(\frac{S_z}{S_N} \right) \right) \end{aligned} \quad (63)$$

where $h = \omega_L/2 = \gamma H/2$ is half the external Larmor frequency.

In order to solve the above equations numerically, we employ the Riccati representation of the quasi-classical Green function. [14, 22, 29, 30] Details are discussed in Appendix B. We obtain the self-consistent order parameter and the spin polarization density by solving the above equations iteratively. For given Δ_{\parallel} , Δ_{\perp} and S_z , we solve the Riccati equations and the surface self energy equations. Using the obtained self energy Σ , we calculate the gap equation and the spin polarization density, and use the results of Δ_{\parallel} , Δ_{\perp} and S_z for the next step.

Typical results are shown in Fig. 2. We have chosen the temperature $T = 0.2T_c$, the cut-off frequency $\omega_c = 30T_c$, the external Larmor frequency $\omega_L = 0.05\pi T_c$, which is about 0.185T when $T_c = 1.828\text{mK}$, and the Fermi liquid parameter $F_0^a = -0.75$. The roughness parameter $W = 1$ corresponds to the diffusive surface and $W = 0.0$ corresponds to the specular surface.

In the bulk region the perpendicular component Δ_{\perp} is smaller than the parallel component Δ_{\parallel} , since the magnetic field is applied perpendicular to the surface. In the vicinity of the surface the profiles of the order parameter are

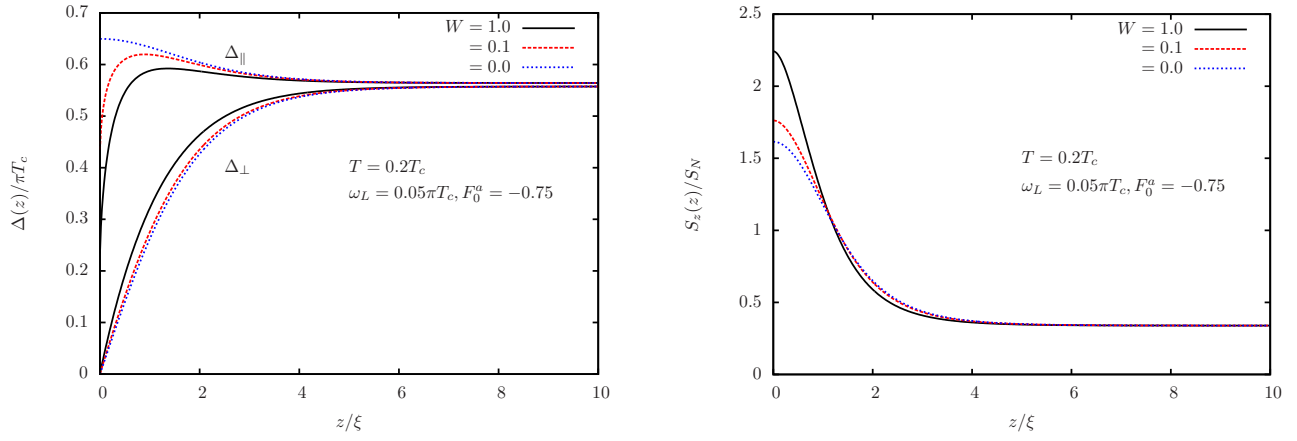


FIG. 2. Self-consistent order parameter $\Delta(z)$ and spin polarization density $S_z(z)$ for some typical values of the roughness parameter W are plotted against the distance from the surface scaled by the coherence length $\xi = v_F/\pi T_c$. $T = 0.2T_c$ and $\omega_L = 0.05\pi T_c$

similar to that of the BW state without magnetic field discussed in our previous paper.[14] The enhancement of the spin polarization density is seen at the surface. At lower temperatures, the enhancement is most pronounced in the diffusive limit $W = 1$. At higher temperatures, however, dependence of the profile on W becomes small.

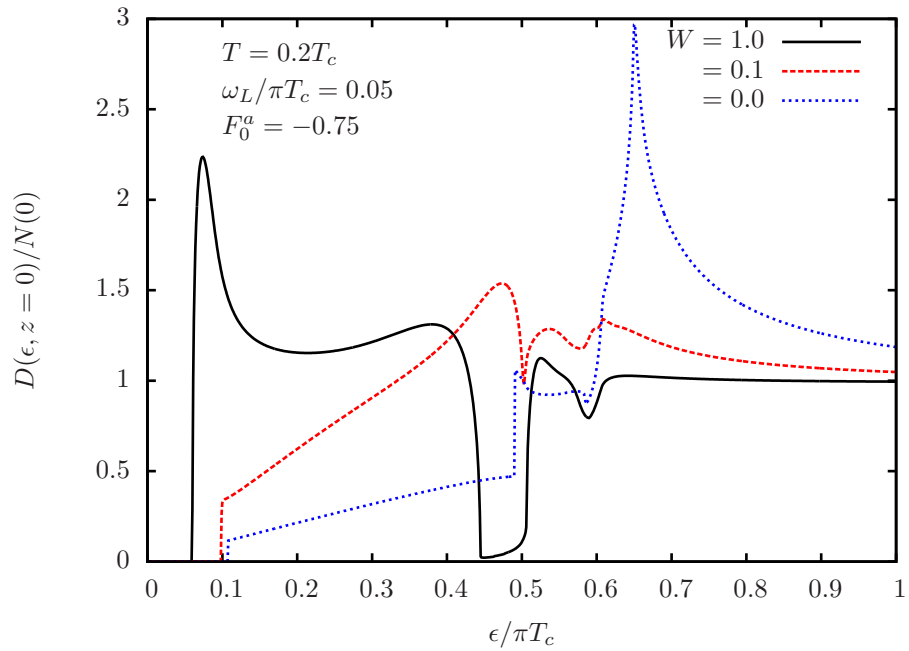


FIG. 3. W dependence of the surface density of states at $T = 0.2T_c$ under the magnetic field $\omega_L = 0.05\pi T_c$.

The surface density of states is calculated from Eqs. (49) and (50). In Fig. 3 we show the W dependence of the surface density of states of $^3\text{He-B}$ at $T = 0.2T_c$ calculated using the self-consistent order parameter and the spin density given in Fig. 2. $W = 0$ corresponds to the specular surface, $W = 1$ to the diffusive limit and $W = 0.1$ corresponds to the surface with specularity factor about 0.5.[14] We find that the “Zeeman gap” Δ_Z decreases with W , as discussed in the previous section. The upper edge Δ^* of the surface bound states band can be seen for any $W \neq 0$. When $W = 1$, well defined subgap structure exists. At $W = 0.1$, however, Δ^* is merged into the continuum spectrum of the Bogoliubov quasi-particle excitations and subgap structure is no longer found.

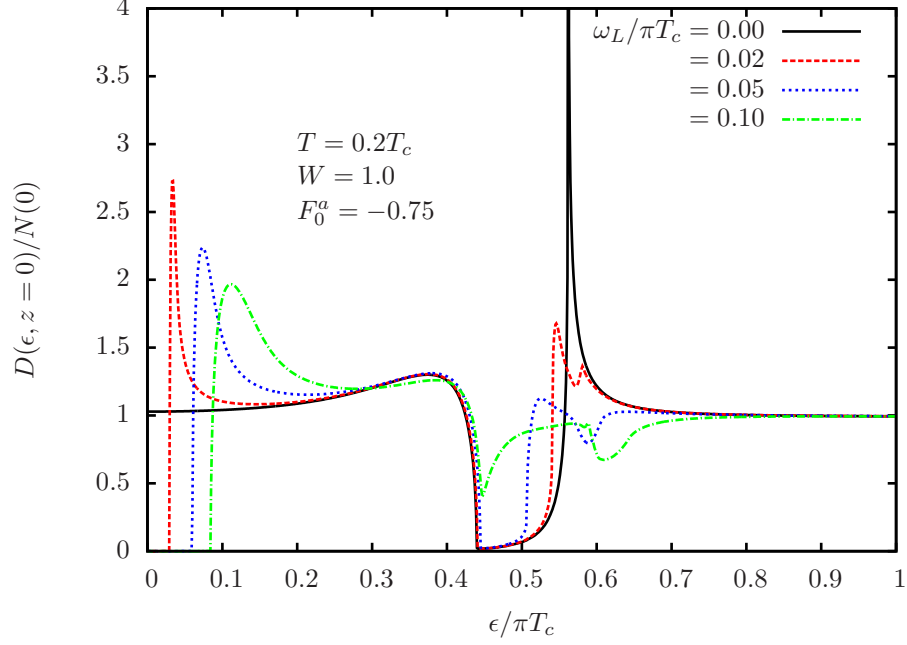


FIG. 4. Surface density of states at $T = 0.2T_c$, $W = 1$ under the magnetic fields $\omega_L = 0.0, 0.02, 0.05$, and $0.10\pi T_c$.

Magnetic field dependence of the surface density of states is shown in Fig. 4. We show the surface density of states at $T = 0.2T_c$ and $W = 1$ under the external magnetic field $\omega_L/\pi T_c = 0.0, 0.02, 0.05$ and 0.10 . The “Zeeman gap” Δ_Z increases with the magnetic field, as it should be. On the other hand the upper edge Δ^* does not so much depend on the magnetic field. The sharp peak at the the bulk energy gap ($\sim 0.5\pi T_c$) that exists when $\omega_L = 0$ is splitted by the magnetic field. This reflects the Zeeman splitting of the Bogoliubov excitations.

As can be seen in Figs. 3 and 4, the surface density of states is characterized by some band edges as well as some peaks. In Fig.5, we plot the surface density of states when $W = 1$, $T = 0.9T_c$ and $\omega_L = 0.03\pi T_c$ together with the bulk density of states. We show the locations of such singularity energies Δ_Z , Δ^* , Δ_- and Δ_+ . Let us discuss on the behavior of those characteristic energies. The energy Δ^* , the upper edge of the surface bound state band, increases toward the bulk energy gap as W decreases.[14] On the other hand, Δ^* depends little on the magnetic field normal to the surface.

The energies Δ_+ and Δ_- are related to the Zeeman splitting of the bulk energy gap. From the quasi-particle energy of the bulk BW state under the magnetic field,[31] we can find

$$\Delta_+ = \begin{cases} \Delta_{\perp b} + \frac{\tilde{\omega}_{Lb}}{2} & \text{for } \Delta_{\parallel b}^2 - \Delta_{\perp b}^2 < \frac{\tilde{\omega}_{Lb}}{2} \Delta_{\perp b} \\ \Delta_{\parallel b} \sqrt{1 + \frac{\tilde{\omega}_{Lb}^2}{4} \frac{1}{\Delta_{\parallel b}^2 - \Delta_{\perp b}^2}} & \text{for } \Delta_{\parallel b}^2 - \Delta_{\perp b}^2 > \frac{\tilde{\omega}_{Lb}}{2} \Delta_{\perp b} \end{cases} \quad (64)$$

$$\Delta_- = \Delta_{\perp b} - \frac{\tilde{\omega}_{Lb}}{2} \quad (65)$$

where the subscript b means the bulk value. As the magnetic field increases, Δ_- decreases. Therefore, when the magnetic field ω_L becomes sufficiently large, Δ_- becomes less than Δ^* and the subgap between Δ^* and Δ_- disappears. This also happens when W is small. When the magnetic field is weak and W is large, the surface states are characterized by the four energies Δ_Z , Δ^* , Δ_- and Δ_+ . In other cases, the surface states are mainly characterized by the two energies Δ_Z and Δ_+ .

“Zeeman gap” Δ_Z is the lower edge of the surface bound state band. Temperature dependence of Δ_Z calculated numerically using the self-consistent order parameter is shown in Fig.6. Δ_Z for the diffusive surface $W \neq 0$ is lowered than that for the specular surface by the level repulsion with the continuum states as discussed in the previous section. In the diffusive limit $W = 1$, Δ_Z decreases with the temperature and becomes continuously to zero at the A-B transition temperature T_{AB} as is shown in the right panel of Fig. 6.

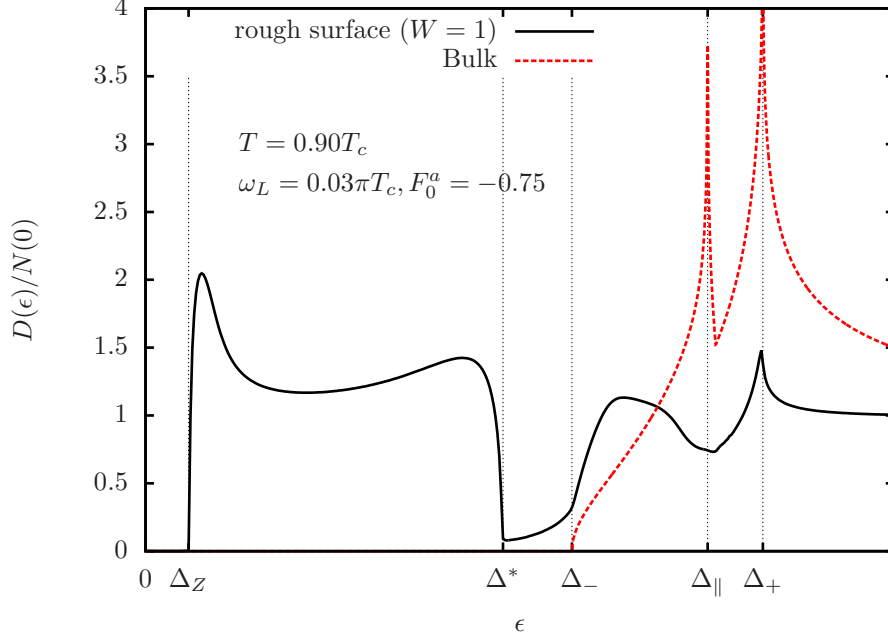


FIG. 5. Characteristic energies $\Delta_Z, \Delta^*, \Delta_-$, and Δ_+ found in the surface density of states. The solid curve shows the local density of states at the rough surface when $T = 0.9T_c, \omega_L = 0.03\pi T_c$. The dashed curve is the density of states in the bulk region.

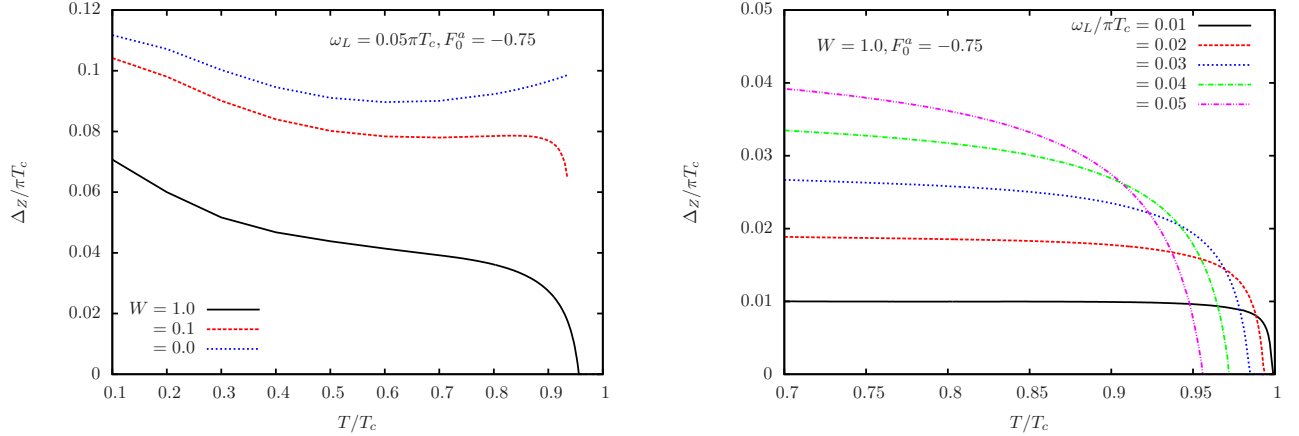


FIG. 6. Temperature dependence of “Zeeman gap” Δ_Z .

VI. TRANSVERSE ACOUSTIC IMPEDANCE

Acoustic impedance is a useful probe to study the surface as well as the bulk properties of neutral liquid ${}^3\text{He}$.^[32] In this section, we consider the transverse acoustic impedance of superfluid ${}^3\text{He-B}$ under the magnetic field normal to the oscillating surface.

We consider the rough wall oscillating in x -direction like $R(t) = Re^{-i\Omega t}$. The acoustic impedance Z is defined by a ratio of the stress tensor Π_{xz} of the liquid at the wall to the velocity \dot{R} of the wall

$$Z \equiv Z' + iZ'' = \frac{\Pi_{xz}}{R(t)} \quad (66)$$

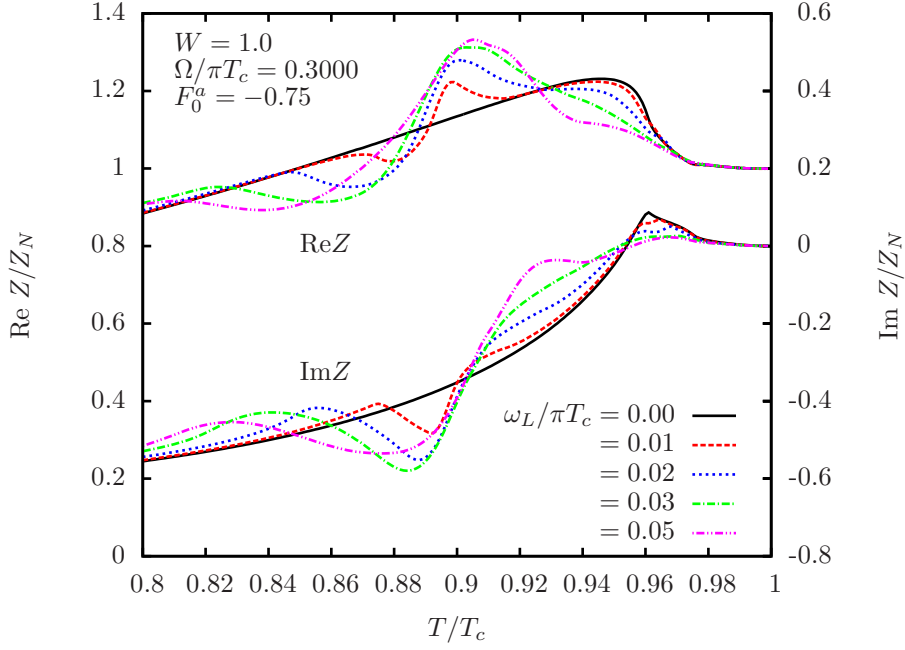


FIG. 7. Temperature dependence of the acoustic impedance Z for a fixed frequency $\Omega = 0.3\pi T_c$.

To study the time dependent problem we use the Keldysh Green function formalism. We have already reported a theory for the system without magnetic field.[5, 13] In case of the magnetic field normal to the surface, we can formulate in almost the same way as the previous report. Some details are discussed in Appendix C. The final expression for the transverse acoustic impedance is given in a form

$$\frac{Z}{Z_N} = \int \frac{d\epsilon}{\Omega} \left(h_- F(\epsilon_+, \epsilon_-)^R - h_+ F(\epsilon_+, \epsilon_-)^A + (h_+ - h_-) F(\epsilon_+, \epsilon_-)^a \right), \quad (67)$$

where $\epsilon_{\pm} = \epsilon \pm \Omega/2$, $h_{\pm} = \tanh(\epsilon_{\pm}/2T)$, Z_N is the normal state impedance in the diffusive limit ($W = 1$). The retarded function F^R , the advanced function F^A and the anomalous function F^a are defined by

$$F^R = F(\epsilon_+ + i0, \epsilon_- + i0), \quad F^A = F(\epsilon_+ - i0, \epsilon_- - i0), \quad F^a = F(\epsilon_+ + i0, \epsilon_- - i0). \quad (68)$$

Explicit form of F is given in Appendix C.

We numerically calculate the acoustic impedance $Z = Z' + iZ''$ using the self-consistent order parameters. In Fig. 7, we show the temperature dependence of the acoustic impedance for a fixed frequency $\Omega = 0.3\pi T_c$ under magnetic fields $\omega_L/\pi T_c = 0.0, 0.01, 0.02, 0.03$ and 0.05 . In the absence of magnetic field, Z is characterized by a kink in the real part Z' and a peak in the imaginary part Z'' at the temperature at which the condition $\Omega = \Delta^*(T) + \Delta_{\text{bulk}}(T)$ is satisfied. It has been shown that the kink-and-peak structure comes from the pair excitations of the bound state and the Bogoliubov quasi-particle.[5, 10, 13] Under finite magnetic fields, the overall temperature dependence of Z' and Z'' are shifted to lower temperature. The peak in the imaginary part Z'' found under zero magnetic field eventually disappears. These behaviors are in agreement with a recent experimental report by Akiyama et al.[33]

At higher magnetic field, the second peak in Z' appears at lower temperature and the impedance shows bumpy structure. The similar bumpy structure can be seen also in the frequency dependence at fixed temperatures. In Fig. 8, we show typical results of the frequency dependence of $Z(\Omega)$ at $T = 0.9T_c$ under various magnetic fields. One can find a large bump around $\Omega = \Delta_{\text{bulk}} \sim 0.3\pi T_c$ when $\omega_L \neq 0$. At lower temperatures, the bumpy structure becomes not so pronounced.

To study the origin of the bumpy structure, we divide the acoustic impedance Z into two parts $Z = Z_1 + Z_2$ by separating the energy integral region in Eq. (67) into $|\epsilon| < \Omega/2$ for Z_1 and $|\epsilon| > \Omega/2$ for Z_2 (see Ref. 5). The component Z_1 and Z_2 give the contribution from the pair excitations and the contribution from the scattering of thermally occupied quasi-particle states, respectively. This can be understood when we look into the real part of Z

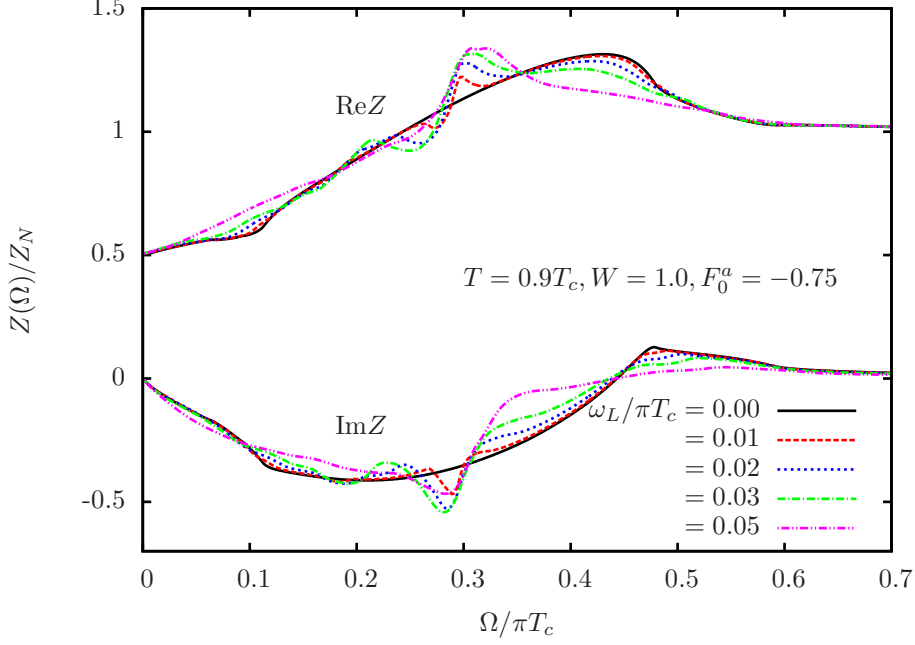


FIG. 8. Frequency dependence of acoustic impedance Z at $T = 0.9T_c$

that is related to the energy absorption.

$$Z'_1/Z_n = \int_{-\Omega/2}^{\Omega/2} \frac{d\epsilon}{\Omega} 2[f(\epsilon_+) + f(|\epsilon_-|) - 1] \left(\frac{F^R + F^A}{2} - \Re F^a \right) \quad (69)$$

$$Z'_2/Z_n = 2 \int_{\infty}^{\Omega/2} \frac{d\epsilon}{\Omega} 2[f(\epsilon_+) - f(|\epsilon_-|)] \left(\frac{F^R + F^A}{2} - \Re F^a \right) \quad (70)$$

where f is the Fermi distribution function. Combination of the Fermi distribution functions implies that Z_1 is from the pair excitations and Z_2 is from the scattering of thermally occupied quasi-particle states.

In Fig. 9 we show the frequency dependence of the separated acoustic impedances under the magnetic field at $T = 0.9T_c$ and $W = 1$. We find that the bump in Z' is formed by a peak in Z'_2 around $\Omega = \Delta_- - \Delta_Z$ and a rapid increase of Z'_1 in the range $\Delta_- + \Delta_Z < \Omega < \Delta_+ - \Delta_Z$. One can also find well defined peak at $\Delta_- - \Delta_Z$ in Z'_2 and at $\Delta_Z + \Delta^*$ in Z'_1 . Precise measurements will provide useful informations for characteristic energies Δ_Z , Δ^* , Δ_- and Δ_+ . One may expect that there exists a jump at $\Omega = 2\Delta_Z$ in the pair excitation spectrum Z'_1 . Unfortunately this is not true because the frequency window $\Delta_Z < \epsilon < \Omega/2$ for Z_1 becomes small at $\Omega = 2\Delta_Z$.

In liquid ^3He , the surface boundary condition for the quasi-particles can be changed by coating the wall by ^4He atoms. It has been suggested that the ^4He film becomes a superfluid and the specularly is enhanced.[8, 11, 12, 34–37] In Fig. 10, we show the temperature dependence of Z under a fixed frequency for several values of surface specularity S which is related to the roughness parameter W . [5, 14] We have chosen $S = 0.0, 0.2, 0.4$ and 0.5 , which correspond to $W = 1.0, 0.264, 0.138$ and 0.1 , respectively. When $S < 0.50$, W is rather small. It follows that the subgap disappears and dominant characteristic energies which remain are Δ_Z and Δ_+ . As indicated by vertical arrows in Fig. 10, we find a small peak in the imaginary part Z'' at the temperature $T(S, \Omega)$ at which $\Omega = \Delta_+(T) - \Delta_Z(T)$ is satisfied. $T(S, \Omega)$ decreases as S increases. This is explained from the fact that $\Delta_+ - \Delta_Z$ is a decreasing function of temperature and also is an increasing function of S because Δ_Z increases with S while Δ_+ is independent of S .

VII. SUMMARY AND DISCUSSION

We have shown that the subgap structure is a result of the interplay between the surface roughness and the surface Majorana state. Subgap structure is also reported in two-dimensional superconductors.[16, 38] Study of the subgap

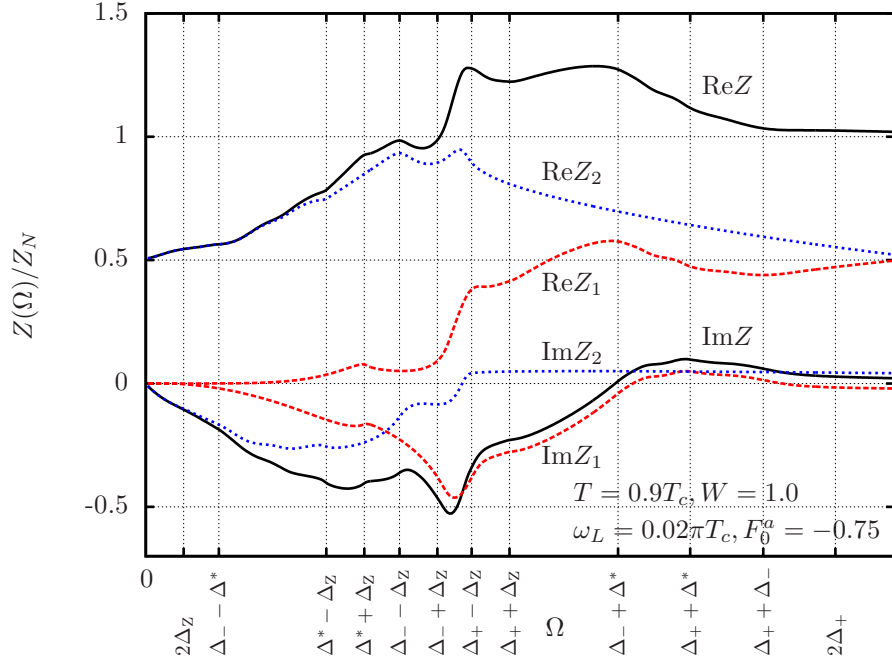


FIG. 9. Separated transverse acoustic impedances. The dashed and dotted lines denote the separated Z_1 and Z_2 components. Upper three curves are real parts and lower three curves are imaginary parts.

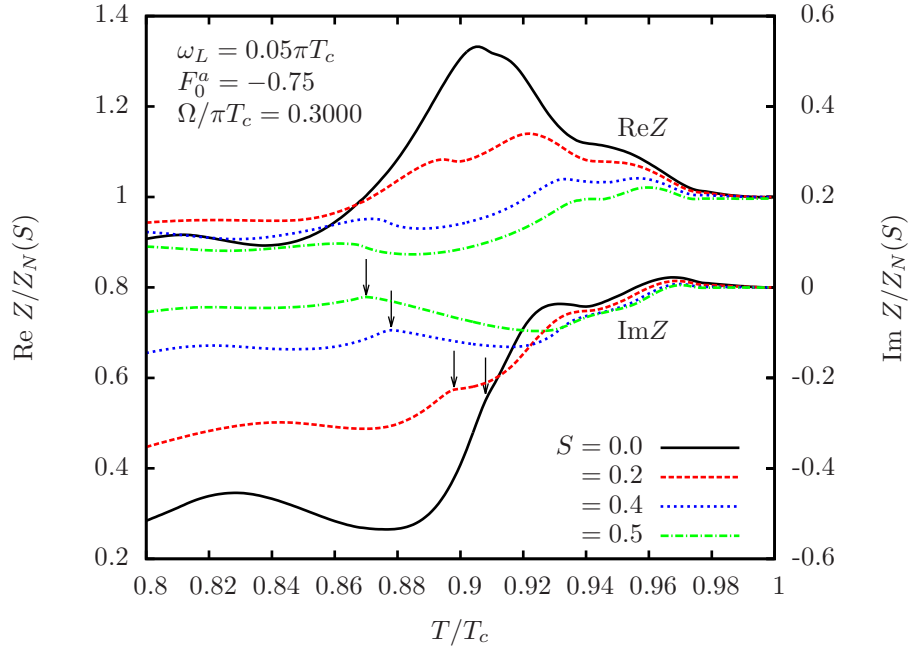


FIG. 10. Temperature dependence of the acoustic impedance Z for several values of specularity S . Z is scaled by the normal state value of the same specularity, $Z_N(S) = Z_N(0)(1 - S)$. Vertical arrow indicates the temperature at which $\Omega = \Delta_+ - \Delta_Z$ for each S .

structure in superfluid $^3\text{He-B}$ and p -wave superconductors will contribute to the further understanding of the surface Majorana Fermions.

In this paper, the surface states of superfluid $^3\text{He-B}$ with a rough plane surface is discussed. We considered the effect by magnetic field applied perpendicular to the surface. We calculated the self-consistent order parameter, spin polarization density and the surface density of states using the quasi-classical Green function theory with the random S -matrix model for the surface roughness.

It was shown that the subgap exists also in $^3\text{He-B}$ under finite magnetic field. The surface density of states is characterized by the ‘‘Zeeman gap’’ Δ_Z , the upper edge of the surface bound states Δ^* , and the Zeeman splitted bulk energy gap Δ_{\pm} . We discussed the dependence of such characteristic energies on the magnetic field, the temperature, and the surface roughness parameter W .

We have also reported the results of numerical calculations of the transverse acoustic impedance and discussed its magnetic field dependence. We found bumpy behavior in the frequency as well as the temperature dependence of the acoustic impedance and discussed how this behavior is related to the surface density of states.

It is a future problem how to detect the ‘‘Zeeman gap’’ Δ_Z experimentally. Recently, using micro-electro-mechanical system (MEMS) devices in $^3\text{He-B}$, Zheng et al.[39, 40] reported an anomalous damping thought to be caused by the surface bound states. It is of great interest how the damping is influenced by magnetic field.

In this paper we considered only the magnetic field perpendicular to the surface. The effect by the magnetic field parallel to the surface is an interesting problem. Quasi-classical theory of the system with magnetic field parallel to the surface has not been fully developed. This will be discussed in a forthcoming paper.

ACKNOWLEDGMENTS

We thank R. Nomura and Y. Okuda for discussion and showing their experimental results before publication. This work was supported in part by JSPS KAKENHI Grant Number JP26400364.

Appendix A: \hat{G}_s for constant order parameter

In this appendix, we show the explicit form of \hat{G}_s at the surface when the order parameter $\Delta_{\parallel}, \Delta_{\perp}$ are constant. Substituting Eq.(25) into Eq. (53), we find \hat{G}_s

$$\hat{G}_{s11} = -\hat{G}_{s44} = \frac{i}{2} \left(\frac{E_+(1 - \epsilon/\sqrt{\epsilon^2 - \Delta_t^2})}{h - \sqrt{\epsilon^2 - \Delta_t^2}} + \frac{E_-(1 + \epsilon/\sqrt{\epsilon^2 - \Delta_t^2})}{h + \sqrt{\epsilon^2 - \Delta_t^2}} \right) \quad (\text{A1})$$

$$\hat{G}_{s22} = -\hat{G}_{s33} = -\frac{i}{2} \left(\frac{E_+(1 + \epsilon/\sqrt{\epsilon^2 - \Delta_t^2})}{h - \sqrt{\epsilon^2 - \Delta_t^2}} + \frac{E_-(1 - \epsilon/\sqrt{\epsilon^2 - \Delta_t^2})}{h + \sqrt{\epsilon^2 - \Delta_t^2}} \right) \quad (\text{A2})$$

$$\hat{G}_{s12} = \hat{G}_{s21} = -\hat{G}_{s34} = -\hat{G}_{s43} = -\frac{\Delta_t \Delta_{\ell}}{\epsilon^2 - (h^2 + \Delta_t^2)} \quad (\text{A3})$$

$$\hat{G}_{s13} = \hat{G}_{s31} = \hat{G}_{s24} = \hat{G}_{s42} = \frac{\Delta_t}{2} \left(\frac{E_+/\sqrt{\epsilon^2 - \Delta_t^2}}{h - \sqrt{\epsilon^2 - \Delta_t^2}} - \frac{E_-/\sqrt{\epsilon^2 - \Delta_t^2}}{h + \sqrt{\epsilon^2 - \Delta_t^2}} \right) \quad (\text{A4})$$

$$\hat{G}_{s14} = \hat{G}_{s41} = i \frac{\Delta_{\ell}(h - \epsilon)}{\epsilon^2 - (h^2 + \Delta_t^2)} \quad (\text{A5})$$

$$\hat{G}_{s23} = \hat{G}_{s32} = -i \frac{\Delta_{\ell}(h + \epsilon)}{\epsilon^2 - (h^2 + \Delta_t^2)}, \quad (\text{A6})$$

where E_{\pm} is given by Eq.(29). It is obvious that \hat{G}_s satisfies Eq.(33)

$$\rho_2 \sigma_1 \hat{G}_s \sigma_1 \rho_2 = -\hat{G}_s \quad (\text{A7})$$

and also \hat{G}_s is a symmetric matrix

$$\hat{G}_s = {}^t \hat{G}_s. \quad (\text{A8})$$

Appendix B: Riccati representation of Quasi-classical Green function

In this appendix, we consider the Riccati representation[14, 22, 29, 30] of the quasi-classical Green function \hat{G}_α and the rough surface boundary condition.

Here we consider \hat{G}_α for $\phi = \pi/2$ ($K_x = 0$) as in section III. The quasi-classical Green's function \hat{G}_+ in the present geometry can be parametrized in terms of 2×2 spin space matrices \mathcal{D}_+ and \mathcal{F}_+ as[30]

$$\hat{G}_+(K, z, \epsilon) = i \begin{pmatrix} 1 & -i\mathcal{F}_+ \\ i\mathcal{D}_+ & 1 \end{pmatrix} \begin{pmatrix} 1 & \\ & -1 \end{pmatrix} \begin{pmatrix} 1 & -i\mathcal{F}_+ \\ i\mathcal{D}_+ & 1 \end{pmatrix}^{-1}. \quad (\text{B1})$$

From the relation $\hat{G}_-(z) = -\rho_2\sigma_1\hat{G}_+(z)\sigma_1\rho_2$ of Eq. (32), we find

$$\hat{G}_-(K, z, \epsilon) = i \begin{pmatrix} 1 & -i\sigma_1\mathcal{D}_+\sigma_1 \\ i\sigma_1\mathcal{F}_+\sigma_1 & 1 \end{pmatrix} \begin{pmatrix} 1 & \\ & -1 \end{pmatrix} \begin{pmatrix} 1 & -i\sigma_1\mathcal{D}_+\sigma_1 \\ i\sigma_1\mathcal{F}_+\sigma_1 & 1 \end{pmatrix}^{-1}. \quad (\text{B2})$$

The matrices \mathcal{D}_+ and \mathcal{F}_+ obey the following Riccati type differential equations

$$-iv_F \cos \theta \partial_z \mathcal{D}_+(z) = (1 \ i\mathcal{D}_+(z)) \rho_2 \mathcal{E}_+ \begin{pmatrix} 1 \\ i\mathcal{D}_+(z) \end{pmatrix} \quad (\text{B3})$$

$$iv_F \cos \theta \partial_z \mathcal{F}_+(z) = (\mathcal{F}_+(z) \ i) \rho_2 \mathcal{E}_+ \begin{pmatrix} \mathcal{F}_+(z) \\ i \end{pmatrix}, \quad (\text{B4})$$

where \mathcal{E}_α is given by Eq. (22)

$$\mathcal{E}_\alpha = \begin{pmatrix} \epsilon + \tilde{h}\tilde{\sigma}_3 & \Delta_\alpha \\ \Delta_{-\alpha} & -\epsilon + \tilde{h}\tilde{\sigma}_3 \end{pmatrix}. \quad (\text{B5})$$

When $\text{Im} \epsilon > 0$, one should solve the Riccati equation for \mathcal{D}_+ in the direction from $z = \infty$ to $z = 0$ and for \mathcal{F}_+ in the opposite direction to have stable solutions. The boundary condition for \mathcal{D}_+ is given at $z = \infty$ by

$$\begin{aligned} i\mathcal{D}_+(\infty) &= (\hat{G}_+^{(0)})_{21} \frac{1}{(\hat{G}_+^{(0)})_{11} + i} \\ &= \frac{i}{\alpha_+\beta_- - \alpha_-\beta_+} \begin{pmatrix} \beta_- - \beta_+ & \alpha_+ - \alpha_- \\ (\alpha_+ - \alpha_-)\beta_+\beta_- & \beta_- - \beta_+ \end{pmatrix}, \end{aligned} \quad (\text{B6})$$

where $\hat{G}^{(0)}$ is the bulk Green's function given by Eq. (25) and

$$\alpha_\pm = \frac{\epsilon \pm \sqrt{\epsilon^2 - \Delta_t^2}}{\Delta_t}, \quad \beta_\pm = i \frac{\tilde{h} \pm \sqrt{\epsilon^2 - \Delta_t^2} - E_\mp}{\Delta_t}.$$

From Eqs. (B3) and (B6), we find that

$$\sigma_1 \mathcal{D}_+(z) \sigma_1 = {}^t \mathcal{D}_+(z). \quad (\text{B7})$$

The boundary condition for \mathcal{F}_+ should be given at $z = 0$. According to the random S-matrix model[14, 22, 23] for the rough surface, \hat{G}_+ and \hat{G}_- satisfy at the surface

$$\hat{G}_-(0) = T \hat{G}_+(0) T^{-1}, \quad T = \frac{1 - i\Sigma}{1 + i\Sigma}, \quad (\text{B8})$$

where Σ is the surface self energy given by Eq.(42). It follows from Eqs. (B1), (B2) and (B8) that at $z = 0$

$$\begin{pmatrix} 1 & -i\sigma_1\mathcal{D}_+\sigma_1 \\ i\sigma_1\mathcal{F}_+\sigma_1 & 1 \end{pmatrix} = T \begin{pmatrix} 1 & -i\mathcal{F}_+ \\ i\mathcal{D}_+ & 1 \end{pmatrix} \begin{pmatrix} A \\ B \end{pmatrix}, \quad (\text{B9})$$

where A, B are constant matrices. The second column reads

$$-i {}^t \mathcal{D}_+ = (T_{11}(-i\mathcal{F}_+) + T_{12}) B \quad (\text{B10})$$

$$1 = (T_{21}(-i\mathcal{F}_+) + T_{22}) B \quad (\text{B11})$$

from which we obtain

$$i\mathcal{F}_+(0) = \frac{1}{T_{11} + i {}^t\mathcal{D}_+(0)T_{21}}(T_{12} + i {}^t\mathcal{D}_+(0)T_{22}) \quad (\text{B12})$$

From the first column, we can obtain an equivalent result by using Eq. (B7) and noting from Eqs. (33) and (42) that the surface self energy Σ can be parametrized in a form

$$\Sigma = \begin{pmatrix} s_{11} & 0 & 0 & s_{14} \\ 0 & s_{22} & s_{23} & 0 \\ 0 & s_{23} & -s_{22} & 0 \\ s_{14} & 0 & 0 & -s_{11} \end{pmatrix}. \quad (\text{B13})$$

We can also show that

$${}^t\mathcal{F}_+(z) = \sigma_1 \mathcal{F}_+(z) \sigma_1. \quad (\text{B14})$$

Finally, \hat{G}_s for the specular surface is given by

$$\hat{G}_s(K, 0, \epsilon) = i \begin{pmatrix} 1 & -i {}^t\mathcal{D}_+(0) \\ i\mathcal{D}_+(0) & 1 \end{pmatrix} \begin{pmatrix} 1 & \\ & -1 \end{pmatrix} \begin{pmatrix} 1 & -i {}^t\mathcal{D}_+(0) \\ i\mathcal{D}_+(0) & 1 \end{pmatrix}^{-1}. \quad (\text{B15})$$

Appendix C: Transverse Acoustic Impedance

We consider the rough wall oscillating in x -direction like $R(t) = Re^{-i\Omega t}$. The acoustic impedance Z is defined by a ratio of the stress tensor Π_{xz} of the liquid at the wall to the velocity \dot{R} of the wall

$$Z = \frac{\Pi_{xz}}{\dot{R}(t)} \quad (\text{C1})$$

To discuss the time dependent problem we use the Keldysh quasi-classical Green's function

$$\check{G}_\alpha(\mathbf{K}, z, t, t') = \begin{pmatrix} \hat{G}_\alpha^R(\mathbf{K}, z, t, t') & \hat{G}_\alpha^K(\mathbf{K}, z, t, t') \\ & \hat{G}_\alpha^A(\mathbf{K}, z, t, t') \end{pmatrix} \quad (\text{C2})$$

We can apply the random S-matrix model for the rough surface to the Keldysh Green function in the same manner as to the equilibrium Green function.[5, 13] To calculate the stress tensor Π_{xz} , we treat the wall displacement $R(t) = Re^{-i\Omega t}$ by perturbation theory. The stress tensor can be calculated from the Keldysh part of the equal time Green function

$$\Pi_{xz} = \sum_{K, \alpha} \frac{1}{2v_K} \frac{1}{2} \text{Tr} \left[K_x \alpha v_K \frac{i}{2} \delta \hat{G}_{\alpha\alpha}^K(K, 0, t, t) \right], \quad (\text{C3})$$

where $v_K = v_F \cos \theta_K$ is the z component of the Fermi velocity. Following the prescription developed in Ref. 13, we obtain

$$\Pi_{xz} = \frac{-1}{4} \sum_K \int \frac{d\epsilon}{2\pi} \text{Tr} \left[\check{\mathcal{G}}(\epsilon_+) \delta \check{\Sigma}(\epsilon_+, \epsilon_-) \check{\mathcal{G}}(\epsilon_-) \check{G}_s(\epsilon_-) - \check{G}_s(\epsilon_+) \check{\mathcal{G}}(\epsilon_+) \delta \check{\Sigma}(\epsilon_+, \epsilon_-) \check{\mathcal{G}}(\epsilon_-) \right]^K, \quad (\text{C4})$$

where $\epsilon_\pm = \epsilon \pm \Omega/2$, $\check{\mathcal{G}}(\epsilon)$, $\check{G}_s(\epsilon)$ are the Fourier transform of the Keldysh Green functions $\check{\mathcal{G}}(t-t')$, $\check{G}_s(t-t')$ in the equilibrium state and

$$\delta \check{\Sigma}(\epsilon, \epsilon') = 2\pi \delta(\epsilon - \epsilon' - \Omega) (\delta \check{\Sigma}^D + \delta \check{\Sigma}^{\text{OD}}), \quad (\text{C5})$$

$$\delta \check{\Sigma}^D = -i K_x R (\check{\Sigma}(\epsilon') - \check{\Sigma}(\epsilon)), \quad (\text{C6})$$

$$\begin{aligned} \delta \check{\Sigma}^{\text{OD}} &= 2iW \langle Q_x R \check{\mathcal{G}}(\epsilon) (\check{G}_s(\epsilon') - \check{G}_s(\epsilon)) \check{\mathcal{G}}(\epsilon') \rangle_Q \\ &\quad + 2W \langle \check{\mathcal{G}}(\epsilon) \delta \check{\Sigma}^{\text{OD}} \check{\mathcal{G}}(\epsilon') \rangle_Q. \end{aligned} \quad (\text{C7})$$

The superscript D (OD) means that the contribution to the impedance comes out through the coupling with the diagonal (off-diagonal) element of $\check{\mathcal{G}}$ in particle-hole space.

Introducing a unitary matrix

$$\hat{\gamma} = \begin{pmatrix} 1 & 0 & 0 & 0 \\ 0 & 0 & 0 & 1 \\ 0 & 0 & 1 & 0 \\ 0 & -1 & 0 & 0 \end{pmatrix}, \quad (\text{C8})$$

we can transform \hat{G}_s , Σ and \mathcal{G} into the form

$$\Sigma = \hat{\gamma}^\dagger \begin{pmatrix} s_1 & 0 \\ 0 & -s_2 \end{pmatrix} \hat{\gamma}, \quad \hat{G}_s = \hat{\gamma}^\dagger \begin{pmatrix} g_1 & g_o e^{-i\phi'} \\ g_o e^{i\phi'} & -g_2 \end{pmatrix} \hat{\gamma} \quad (\text{C9})$$

$$\mathcal{G} = [\hat{G}_s^{-1} - \Sigma]^{-1} = \hat{\gamma}^\dagger \begin{pmatrix} \mathcal{G}_1 & \mathcal{G}_o e^{-i\phi'} \\ \mathcal{G}_o e^{i\phi'} & -\mathcal{G}_2 \end{pmatrix} \hat{\gamma} \quad (\text{C10})$$

where $\phi' = \phi_K - \pi/2$. This can be shown from the properties of \hat{G}_s given by Eqs. (20) and (32) and also from Eq. (B13) for Σ . Substituting them into Eqs. (C4), we can analytically perform the ϕ_K average. We finally obtain the expression for the transverse acoustic impedance.

$$Z/Z_N = \int_{-\infty}^{\infty} d\epsilon \frac{1}{\Omega} [F^R(\epsilon_+, \epsilon_-) h_- - F^A(\epsilon_+, \epsilon_-) h_+ + F^a(\epsilon_+, \epsilon_-) (h_+ - h_-)] \quad (\text{C11})$$

where Z_N is the normal state impedance and $h_{\pm} = \tanh(\beta\epsilon_{\pm}/2)$. The retarded, advanced and anomalous functions $F^{R,A,a}$ are given by

$$F^R = F(\epsilon_+ + i0, \epsilon_- + i0), \quad F^A = F(\epsilon_+ - i0, \epsilon_- - i0), \quad F^a = F(\epsilon_+ + i0, \epsilon_- - i0). \quad (\text{C12})$$

The explicit form of F is given as follows.

$$F(\epsilon_+, \epsilon_-) = F^D(\epsilon_+, \epsilon_-) + F^{OD}(\epsilon_+, \epsilon_-) \quad (\text{C13})$$

$$F^D = \left\langle \sin^2 \theta \frac{1}{4} \text{Tr} [(s'_1 - s_1) a_1 + (s'_2 - s_2) a_2] \right\rangle_{\theta} \quad (\text{C14})$$

$$F^{OD} = \left\langle \sin \theta \frac{1}{4} \text{Tr} [\bar{\zeta} b_1 - \bar{\eta} b_2] \right\rangle_{\theta} \quad (\text{C15})$$

$$a_1 = \mathcal{G}_1(g'_1 - g_1)\mathcal{G}'_1 + \mathcal{G}_1(g'_o - g_o)\mathcal{G}'_o + \mathcal{G}_o(g'_o - g_o)\mathcal{G}'_1 - \mathcal{G}_o(g'_2 - g_2)\mathcal{G}'_o \quad (\text{C16})$$

$$a_2 = \mathcal{G}_2(g'_2 - g_2)\mathcal{G}'_2 + \mathcal{G}_2(g'_o - g_o)\mathcal{G}'_o + \mathcal{G}_o(g'_o - g_o)\mathcal{G}'_2 - \mathcal{G}_o(g'_1 - g_1)\mathcal{G}'_o \quad (\text{C17})$$

$$b_1 = \mathcal{G}_1(g'_1 - g_1)\mathcal{G}'_o + \mathcal{G}_o(g'_o - g_o)\mathcal{G}'_o - \mathcal{G}_1(g'_o - g_o)\mathcal{G}'_2 + \mathcal{G}_o(g'_2 - g_2)\mathcal{G}'_2 \quad (\text{C18})$$

$$b_2 = \mathcal{G}_o(g'_1 - g_1)\mathcal{G}'_1 + \mathcal{G}_o(g'_o - g_o)\mathcal{G}'_o - \mathcal{G}_2(g'_o - g_o)\mathcal{G}'_1 + \mathcal{G}_2(g'_2 - g_2)\mathcal{G}'_o \quad (\text{C19})$$

Here s, g, \mathcal{G} with prime are functions of ϵ_- while s, g, \mathcal{G} without prime are functions of ϵ_+ . Corresponding to Eq. (C7) for $\delta\tilde{\Sigma}^{OD}$ we should solve the following equations for $\bar{\zeta}$ and $\bar{\eta}$

$$\bar{\zeta} = -2W \langle \mathcal{G}_1 \bar{\zeta} \mathcal{G}'_2 \rangle_{\theta} - W \langle \sin \theta b_1 \rangle_{\theta} \quad (\text{C20})$$

$$\bar{\eta} = -2W \langle \mathcal{G}_2 \bar{\eta} \mathcal{G}'_1 \rangle_{\theta} + W \langle \sin \theta b_2 \rangle_{\theta}, \quad (\text{C21})$$

where

$$\langle \cdots \rangle_{\theta} = 2 \int_0^{\pi/2} d\theta \sin \theta \cos \theta \cdots \quad (\text{C22})$$

-
- [1] V. Ambegaokar, P. G. de Gennes and D. Rainer, Phys. Rev. A **9**, 2676 (1974).
[2] L. J. Buchholtz and G. Zwirner, Phys. Rev. B **23**, 5788 (1981).
[3] J. Hara and K. Nagai, Prog. Theor. Phys. **76**, 1237 (1986).
[4] W. Zhang, Phys. Lett. A **130**, 314 (1988).
[5] K. Nagai, Y. Nagato, M. Yamamoto and S. Higashitani, J. Phys. Soc. Jpn **77**, 111003 (2008).

- [6] A. P. Schnyder, S. Ryu, A. Furusaki and A. W. W. Ludwig: Phys. Rev. B **78** (2008) 195125.
- [7] X.-L. Qi, T.L. Hughes, S. Raghu and S.-C.Zhang: Phys. Rev. Lett. **102** (2009) 187001.
- [8] Y. Okuda and R. Nomura, J. Phys.: Condensed Matter **24**, 343201 (2012).
- [9] T. Mizushima, Y. Tsutsumi, T. Kawakami, M. Sato, M. Ichioka, and K. Machida, J. Phys. Soc. Jpn **85**, 022001 (2016).
- [10] Y. Aoki, Y. Wada, R. Nomura, Y. Okuda, Y. Nagato, M. Yamamoto, S. Higashitani and K. Nagai, Phys. Rev. Lett. **95**, 075301 (2005).
- [11] S. Murakawa, Y. Tamura, Y. Wada, M. Wasai, M. Saitoh, Y. Aoki, R. Nomura, Y. Okuda, Y. Nagato, M. Yamamoto, S. Higashitani and K. Nagai, Phys. Rev. Lett. **103** , 155301 (2009).
- [12] S. Murakawa, Y. Wada, Y. Tamura, M. Wasai, M. Saitoh, Y. Aoki, R. Nomura, Y. Okuda, Y. Nagato, M. Yamamoto, S. Higashitani and K. Nagai, J. Phys. Soc. Jpn **80** , 013602 (2011).
- [13] Y. Nagato, M. Yamamoto, S. Higashitani and K. Nagai, J. Low Temp. Phys. **149**, 294 (2007).
- [14] Y. Nagato, M. Yamamoto and K. Nagai, J. Low Temp. Phys. **110**, 1135 (1998).
- [15] A. B. Vorontsov and J. A. Sauls, Phys. Rev. B **68**. 064508 (2003).
- [16] Y. Nagato, S. Higashitani and K. Nagai, J. Phys. Soc. Jpn **80**, 113706 (2011).
- [17] Y. Nagato, S. Higashitani and K. Nagai, J. Phys. Soc. Jpn, **78**, 123603 (2009).
- [18] S. B. Chung and S.-C. Zhang, Phys. Rev. Lett. **103**, 235301 (2009).
- [19] G. E. Volovik, Pm Zh. Eksp. Teor. Fiz. **90**, 587, (2009).
- [20] T. Mizushima and K. Machida, J. Low Temp. Phys. **162**, 204 (2011).
- [21] M. A. Silaev, Phys. Rev. B **84**, 144508 (2011).
- [22] Y. Nagato, S. Higashitani, K. Yamada and K. Nagai, J. Low Temp. Phys. **103**, 1 (1996).
- [23] K. Nagai, in *Quasiclassical Methods in Superconductivity and Superfluidity*, edited by D. Rainer and J.A. Sauls (Verditz, Bayreuth, Germany 1996)
- [24] M. Ashida, S. Aoyama, J. Hara and K. Nagai, Phys. Rev. B **40**, 8673 (1989)
- [25] Yu. N. Ovchinnikov, Sov. Phys. JETP **29**, 853 (1969).
- [26] N. B. Kopnin, J. Low Temp.Phys. **85**, 267 (1991).
- [27] Y. Nagato, K. Nagai and J. Hara, J. Low Temp. Phys **93**, 33 (1993)
- [28] S. Higashitani and K. Nagai, J. Phys. Soc. Jpn **64**, 549 (1995)
- [29] N. Schopohl and K. Maki, Phys. Rev. B **52** 490 (1995)
- [30] M. Eschrig, Phys. Rev. B **61** 9061 (2000).
- [31] M. Ashida and K. Nagai, Prog. Theor. Phys. **74**, 949 (1985).
- [32] W.P. Halperin and E. Varoquaux, in *Helium Three*, ed. by W.P. Halperin and P.L. Pitaevski (Elsevier, Amsterdam,1990), p.353.
- [33] K. Akiyama, M. Wasai, M. Mashino, T. Nakao, S. Murakawa, R. Nomura and Y. Okuda, J. Phys. Soc. Jpn **84**, 065001 (2015).
- [34] M. R. Freeman and R. C. Richardson, Phys. Rev. B **41** , 11011 (1990).
- [35] S. M. Tholen and J. M. Parpia, Phys. Rev. Lett. **68** 2810 (1992).
- [36] D. Kim, M. Nakagawa, O. Ishikawa, T. Hata, T. Kodama and H. Kojima, Phys. Rev. Lett. **71**, 1581 (1993).
- [37] S. Murakawa, M. Wasai, K. Akiyama, Y. Wada, Y. Tamura, R. Nomura and Y. Okuda, Phys. Rev. Lett. **108**, 025302 (2012).
- [38] S. V. Bakurskiy, A. A. Golubov, M. Yu. Kupriyanov, K. Yada and Y. Tanaka, Phys. Rev. B **90**, 064513 (2014).
- [39] P. Zheng, W. G. Jiang, C. S. Barquist, Y. Lee, and H. B. Chan, Phys. Rev. Lett. **117**, 195301 (2016).
- [40] P. Zheng, W. G. Jiang, C. S. Barquist, Y. Lee, and H. B. Chan, Phys. Rev. Lett. **118**, 065301 (2017).